Data and Metadata. 2025; 4:768
doi: 10.56294/dm2025768

ORIGINAL

Effect of 3D printing parameters on the mechanical characteristics of carbon fiber-reinforced PLA

Efecto de los parámetros de impresión 3D en las características mecánicas del PLA reforzado con fibra de carbono

Arley Chuquin[1], Brizeida Gámez[1], Marco Naranjo[1], David Ojeda[1]

[1]Universidad Técnica del Norte, Facultad de Ingeniería en Ciencias Aplicadas. Ibarra, Ecuador.

Cite as: Chuquin A, Gámez B, Naranjo M, Ojeda D. Effect of 3D printing parameters on the mechanical characteristics of carbon fiber-reinforced PLA. Data and Metadata. 2025; 4:768. https://doi.org/10.56294/dm2025768

Submitted: 11-05-2024 **Revised:** 14-09-2024 **Accepted:** 29-03-2025 **Published:** 30-03-2025

Editor: Dr. Adrián Alejandro Vitón Castillo

Corresponding Author: Brizeida Gámez

ABSTRACT

The comparative results of the mechanical behavior of carbon fiber-reinforced Polylactic Acid (PLA FC) specimens of two brands of filaments for printing by the Fused Deposition Modeling (FDM) process are presented. The experiments were carried out according to ASTM D638 14, using Type I specimens with the established dimensions. For the generation of the 3D model, parameters such as printing temperature, printing speed, density, and filling pattern were set. Cubic, gyroid, and triangular filling patterns were used, with filling densities of 40 %, 60 %, and 80 %. For each configuration, a G-code was generated and used for the fabrication of each specimen. A total of 90 specimens were used, which were divided into two groups according to the brand. Subsequently, tensile tests were carried out to determine the mechanical properties by analyzing the stress-strain curves under the established conditions. Comparative analysis revealed that SUNLU's PLA FC filament achieves higher ultimate stress values, while Artillery's filament has a better ability to withstand deformation. Likewise, the filler pattern that withstood the greatest load was the cubic one.

Keywords: Carbon Fiber-Reinforced PLA; Ultimate Stress; Deformation; Filament; Filling Pattern.

RESUMEN

Se presentan los resultados comparativos del comportamiento mecánico en probetas de Ácido Poliláctico reforzado con Fibra de Carbono (PLA FC) de dos marcas, de filamentos para impresión mediante el proceso de Modelado por Deposición Fundida (FDM). Los experimentos se llevaron a cabo de acuerdo con la norma ASTM D638 14, utilizando probetas Tipo I con las dimensiones establecidas. Para la generación del modelo 3D, se establecieron parámetros como la temperatura de impresión, velocidad de impresión, densidad y patrón de relleno. Se emplearon patrones de relleno cúbico, giroide y triangular, con densidades de relleno del 40 %, 60 % y 80 %. Para cada configuración se generó un código G el cual se utilizó para la fabricación de cada probeta. Se utilizaron un total de 90 especímenes, que se dividieron en dos grupos según la marca. Posteriormente, se llevaron a cabo ensayos a tracción para determinar las propiedades mecánicas, analizando las curvas de esfuerzo-deformación bajo las condiciones establecidas. El análisis comparativo reveló que el filamento de PLA FC de SUNLU alcanza mayores valores de esfuerzo último, mientras que el filamento de Artillery posee una mejor capacidad para soportar deformación. Así mismo, el patrón de relleno que soportó mayor carga fue el cúbico.

Palabras clave: PLA Reforzado con Fibra de Carbono; Esfuerzo Último; Deformación; Filamento; Patrón de Relleno.

INTRODUCTION

The 3D printing process using fused deposition modeling (FDM) is an additive manufacturing technology. It is one of the most widely used manufacturing techniques in producing complex parts in various engineering applications. It is an advanced and efficient process through which three-dimensional components of complex geometry can be manufactured with negligible material waste. The advantages of 3D printing are distinguished from other technologies by its profitability, low equipment costs, reduction of waste, and handling of complex geometries; however, these benefits are not fully recognized, which limits its definitive penetration in the market. Filaments made of composite polymeric materials have reported superior performance in printed parts. Fiber-reinforced polymeric composite materials have been the subject of research for developing additive products in recent years.

Venkateswar and other researchers evaluated the importance of different printing parameters, such as infill density, printing speed, and layer thickness, regarding the tensile strength of components printed in 3D using the fused deposition modeling (FDM) technique. It was determined that tensile strength is significantly affected by nozzle temperature and an increase in printing speed, which leads to a reduction in mechanical properties; however, it was observed that there is more excellent adhesion between layers and better distribution of the material in parts with thinner layers and higher densities.

On the other hand, the desired tensile strength of carbon fiber-reinforced polylactic acid (PLA) was determined by optimizing various printing parameters using the Taguchi L9 experimental design. Nine test specimens were manufactured according to the ASTM standard, resulting in an optimum tensile strength of 21,961 MPa. The process parameters are 80 % filling density, 80 mm/s printing speed, and 100 µm layer height.

In another piece of research, carbon fiber reinforced PLA composites were characterized using the FDM technique, for which four groups of test pieces were prepared: thermoplastic of Polylactic Acid (PLA), PLA with Short Carbon Fiber (PLA-SCF), PLA printed with Continuous Carbon Fiber (PLA-CCF) and PLA-SCF printed with CCF (PLA-SCF-CCF), in which the effects on the tensile and flexural properties of the samples after their manufacturing process were studied experimentally. The CCF-reinforced PLA composite showed the highest tensile strength and Young's modulus of 245,40 MPa and 27,93 GPa, respectively. The PLA-CCF samples showed the highest average flexural stress value of 168,88 MPa. In addition, the optical micrograph of the impregnated carbon fiber cross-section confirms the existence of resin and CCF with some air voids.

Additionally, the results of the mechanical properties of test pieces for a particular type of Continuous Fiber Reinforced Thermoplastic Composites (CFRTPC) were analyzed: nylon matrix Reinforced with Continuous Carbon Fibers (CRTP), Kevlar (KvRTP), and fiberglass (FGRTP), which were manufactured by fused deposition modeling (FDM). The experiments reported are tension, flexion, and shear, where the fibers were oriented at 45° from the load axis. The orientation and fiber content significantly influence the mechanical properties of additively manufactured composite materials. Concentric fiber deposition was discovered to have a lower mechanical performance than the isometric option.

Likewise, the effect of the orientation of the construction, the thickness of the layer, and the volume content of the fiber on the mechanical performance of 3D printed continuous fiber reinforced composite components was characterized. Tensile and three-point bending tests were performed to determine the mechanical response of the printed test pieces. The effect of the thickness of the layer of nylon samples on the mechanical performance was marginally significant. In addition, the continuous fiber-reinforced samples show higher strength and stiffness values than the unreinforced ones. The results show that carbon fiber-reinforced composites exhibit the best mechanical performance with higher stiffness.

On the other hand, the mechanical properties related to hardness, surface roughness, and visualization of the microstructure of Acrylonitrile (ABS), Glycol-modified Polyethylene Terephthalate (PETG), and PLA test specimens were determined using the FDM technique by ASTM specifications. The diamond pattern specimen had an extreme hardness of 16,4 HB for ABS material, a slightly different hardness of 15,8 HB for PLA, and a minimum hardness of 10HB for PETG.

In addition, the mechanical properties and interlaminar fracture toughness of carbon fiber-reinforced polyamide (CF/PA) were investigated. For the case of longitudinal traction, two types of specimen geometries were considered by ASTM D638 and ASTM D3039. The results show that the specimens under the D638 standard fail prematurely due to the concentration of stresses and irregularity at the starting point of the 3D printing. The samples under the D3039 standard are the best option to characterize the longitudinal properties of this material because their results are more consistent, with deformations at failure of around 12,6 %. Monolithic CF/PA samples without any additional reinforcement were used to characterize interlaminar fracture toughness. The results show that prismatic specimens with paper tabs are more appropriate for describing the material properties. Using thick specimens for fracture toughness testing complicates the characterization and can lead to erroneous results.

The different kenaf proportions were also explored, as these impact the strength characteristics of the PLA 2003D filament used in 3D printing. The analysis began by extruding the Ingeo NatureWorks PLA 2003D pellet

https://doi.org/10.56294/dm2025768

at a temperature of 190 °C and a screw speed of 7 rpm. The 3D prints were made with a filling pattern of 90° frame angle and a filling density of 100 %. According to ASTM D638, mechanical tests were used to evaluate the quality of the extruded PLA filament. It was observed that a kenaf fiber load of 15 % showed the best tensile properties among the different filler loads, evidencing an improvement in the tensile properties of the filament with the addition of kenaf fiber as reinforcement.

On the other hand, the impact of FDM process parameters using Polylactic Acid (PLA) was investigated. An experimental design using the Box-Behnken approach was used, and multiple sets of PLA samples were produced using various FDM process parameters, including air gap, extruder temperature, layer thickness, infill density, and weft angle. The tensile strength of each sample was measured using a universal testing machine. A maximum tensile strength of 18,48 MPa was obtained in sample 39 under a load of 3,69 kN, and a minimum tensile strength of 2,72 MPa in sample 37. The results indicate that the specific process parameters in the fused deposition modeling (FDM) technique significantly affect tensile strength.

Finally, the influence of three specific variables of the printing process was detailed: raster angle (RSA), layer thickness (LYT), and infill density (IFD), in two fundamental aspects: fracture resistance and behavior against deformation in samples printed using PLA. An extensive experimental study incorporated 27 different printing process combinations, totaling 108 test specimens evaluated. In addition, two quadratic mathematical models were developed to predict the tensile strength and deformation at the moment of fracture in the printed test specimens, considering the influence of the printing parameters. The results obtained from the prediction were compared favorably with the experimental results. Finally, the study presented an optimized set of printing parameters recommended to improve the durability and integrity of the manufactured parts.

The processes of obtaining printed parts using FDM technology are widely used in Ecuador; however, it is necessary to consider the changes in properties that the filament materials undergo according to the printing parameters established by the manufacturer. Given the above, this research aims to evaluate the influence of different 3D printing parameters on the mechanical properties of carbon fiber-reinforced PLA test pieces marketed in Ecuador.

METHOD

Below are the parameters considered for the tensile testing of the specimens and the specifications for conducting the tests. The results are then presented to analyze the mechanical behavior of the PLA-FC filament specimens.

Experiment specifications

Type of test: tensile test.

Standard: ASTM D638-14 with Type I specimen.

Universal testing machine: the James Heal Titan 5kN dynamometer, which belongs to the Textile Engineering degree, is used.

Filament brands: PLA-FC SUNLU and PLA-FC Artillery

Printing parameters:

- Fill density: fill densities of 40 %, 60 % and 80 % are established.
- Fill pattern: cubic, gyroid, and triangular patterns are used.
- Printing speed: the speed is set at 60 mm/s.
- Printing temperature: the temperature is set at 210°C.
- Printing plate temperature: a temperature of 60°C is used.

Specimen design

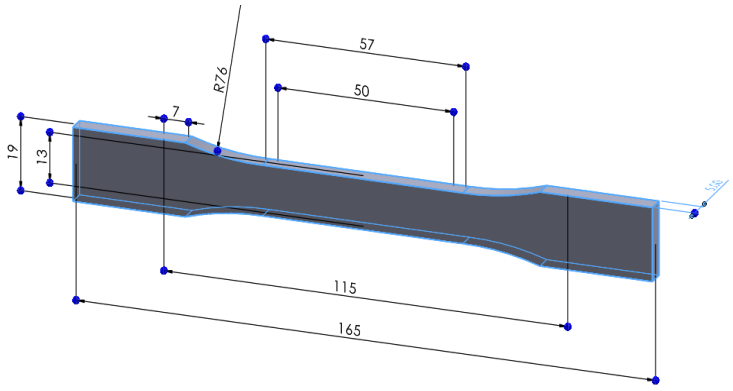

Figure 1. 3D model of the Type I test tube

https://doi.org/10.56294/dm2025768

The dimensions of the specimen are based on ASTM D638-14—the profile for the Type I specimen was used with its respective dimensions (figure 1).

Printing parameters

The 3D printing parameters configured for this experiment are shown in table 1.

Table 1. Print settings in Ultimaker CURA software

Configuration	Parameters	PLA FC (SUNLU y Artillery)
Quality	Layer height	0,2 mm
Walls	Wall thickness	0,84 mm
	Wall line count	2
	Top thickness	0,8 mm
	Top layers	4
	Bottom thickness	0,8 mm
	Bottom layers	4
Filling	Fill density	40 %, 60 %, 80 %
	Fill pattern	Cubic, Gyroid, Triangular
Material	Printing temperature	210 °C
	Printing plate temperature	60 °C
	Filament diameter	1,75 mm
Speed	Printing speed	60 mm/s
	Initial layer speed	45 mm/s
Refrigeration	Fan speed	100 %

Printing and classifying the test tubes

Once the printing parameters have been established in the Ultimaker Cura software, the G-code file of the test tube must be saved on a USB memory stick, which must be inserted into the 3D printer for manufacturing. Then, the file to be printed is selected, and the printer heats the nozzle to 140 °C and the printing plate to 60 °C. When both parameters are at their value, the nozzle temperature rises to 210 °C, and printing the specimen layer by layer begins.

Given the established configuration, four lower layers are printed, followed by other layers and four upper layers according to the filling pattern. Five test tubes are printed with three infill patterns and three infill density percentages, giving 90 test tubes, 45 PLA-FC SUNLU test tubes, and 45 PLA-FC Artillery test tubes. The printing time varies between 40 min and one hour 39 min. Once the printing is finished, it is necessary to wait at least 10 min before removing the test piece. Then, they are classified according to the filling pattern, density, and brand, and the length of the narrow section is marked in white.

Tensile test of PLA-FC specimens

The James Heal Titan machine, which has a maximum load capacity of 5000 N, is used to carry out the tests, and the following steps are required:

- Configure the parameters in the TestWise software, which is linked to the testing machine (table 2).
- Subsequently, each specimen must be secured in the upper and lower grips, verifying that it is aligned in the direction in which the test will be carried out (figure 2).
- The software generates a report with the Force-Extension curves of each specimen subjected to the test.

Table 2. TestWise software configuration

Parameters	Configuration
Speed of the test	50 mm/min
Number of test tubes per group	5
Direction	Urdimbre

https://doi.org/10.56294/dm2025768

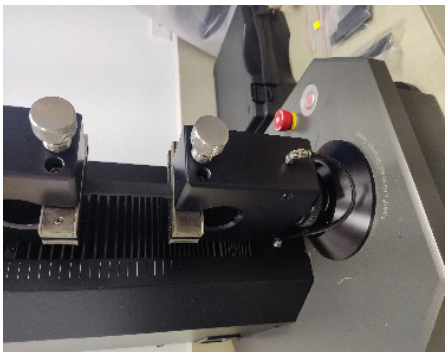

Figure 2. Placing the test piece in the testing machine

Calculations

After having completed the tensile tests, the results for each group of test specimens must be analyzed. For which equation 1 is used.

$$\sigma = \frac{P}{A_T} \qquad (1)$$

The strength (P) is obtained from the report exported by the software for each specimen. The area (AT) of the cross-section of the specimen depends on the upper and lower layers, walls, pattern and packing density, as shown in figure 3.

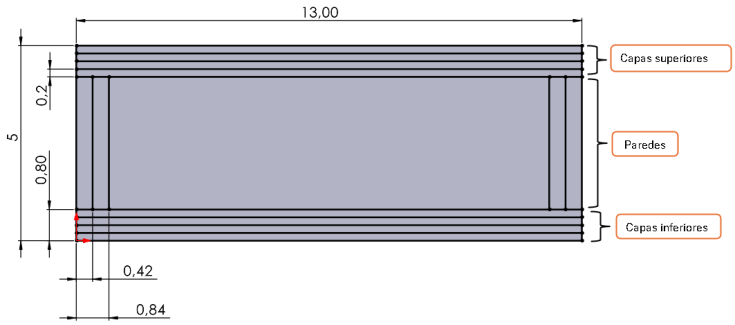

Figure 3. Cross-section of the test piece

Due to the configuration of the test tubes, it is necessary to determine the area equivalent to the upper and lower layers, defined as ASI, and calculated using equation 2.

$$A_{SI} = L_c \times h_c \times n_c \qquad (2)$$

Where:
A_{SI}: area of the upper and lower layers [mm2].
L_c: length of the layer [mm].
h_c: layer height [mm].
n_c: number of layers.

To calculate the area of the walls, equation 3 is used.

$$A_p = L_p \times h_p \times n_p \qquad (3)$$

Where:
A_p: wall area [mm2].
L_p: wall length [mm].
h_p: wall height [mm].
n_p: number of walls.

To obtain the area that remains constant for each test tube, equation 4 is used:

https://doi.org/10.56294/dm2025768

$$A_1 = A_{SI} + A_p \qquad (4)$$

Where:
A_1: constant area [mm2].
A_{SI}: area of the upper and lower layers [mm2].
A_p: wall area [mm2].

By way of example, figure 4 shows the internal configuration of the cross-section of the test piece with an 80 % gyroid filling pattern.

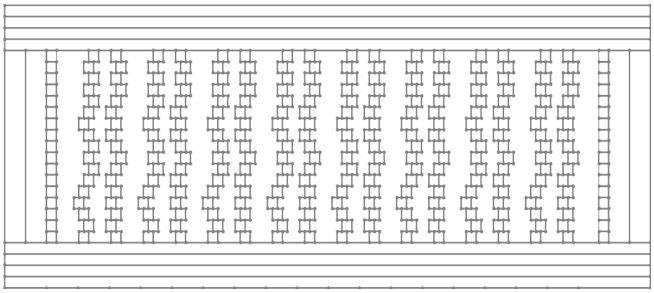

Figure 4. Cross-section of the test piece with a gyroid filling pattern and 80 % density

To calculate the area of the internal configuration, we must reconstruct the cross-section layer by layer using the Ultimaker Cura software. We consider the number of internal layers and the number of squares where the thickness of the filling layer and the layer height are 0,2 mm; therefore, the area of each square is 0,04 mm2. Then, we proceed to calculate the internal area using equation 5

$$A_2 = A_{\blacksquare} \times N_{\blacksquare} \qquad (5)$$

Where:
A_2: internal configuration area [mm2].
$A_{\blacksquare}$: area of each square [mm2].
$N_{\blacksquare}$: number of squares.

To calculate the total cross-sectional area, equation 6 is used:

$$A_T = A_1 + A_2 \qquad (6)$$

Where:
A_T: total cross-sectional area [mm2].
A_1: constant area [mm2].
A_2: internal configuration area [mm2].

Table 3 shows the results obtained using equations 2-6 for all the patterns and fill densities.

Table 3. Cross-sectional area of the test pieces

Area of the test tube [mm²]	Fill pattern								
	Cubic			Gyroid			Triangular		
	40 %	60 %	80 %	40 %	60 %	80 %	40 %	60 %	80 %
A_1 [mm²]	26,51	26,51	26,51	26,51	26,51	26,51	26,51	26,51	26,51
A_2 [mm²]	4,96	6,84	8,32	6,68	9,44	12,24	5,2	6,12	9,52
A_T [mm²]	31,47	33,35	34,83	33,19	35,95	38,75	31,71	32,63	36,03

Then, the deformation is calculated when maximum tensile strength is obtained using equation (7).

$$\varepsilon = \frac{l_f - l_0}{l_0} \qquad (7)$$

Where:
Corresponds to the final length of the test piece and is the original length (before the test) of the test piece.

RESULTS

The results are shown based on the tensile tests of the specimens made with PLA-FC filaments of the SUNLU and Artillery brands and densities of 40 %, 60 %, and 80 %. For each group of test specimens, the mechanical properties and stress-strain curves are presented, with the standard deviation (SD) as a measure of data dispersion and the median (M) as a representative value. In all cases, the test specimens were divided into narrow sections, the limits of which are marked with white lines.

SUNLU PLA-FC test pieces

Tables 4, 5, 6 and figures 5, 6 and 7 show the results of the tensile test on SUNLU test pieces with cubic, gyroid and triangular packing patterns, respectively.

Table 4. Tensile test results for cubic PLA-FC (SUNLU) test pieces

P	Maximum Strength (N)			Extension (mm)			Last-ditch effort (MPa)			Deformation (mm/mm)		
	40 %	60 %	80 %	40 %	60 %	80 %	40 %	60 %	80 %	40 %	60 %	80 %
1	1279	1421	1644	5,115	5,252	5,705	40,65	42,61	47,19	0,06367	0,06536	0,07115
2	1283	1438	1630	5,253	5,251	5,623	40,77	43,13	46,81	0,06539	0,06535	0,07012
3	1311	1450	1722	5,336	5,256	5,796	41,67	43,48	49,45	0,06642	0,06541	0,07229
4	1293	1481	1759	5,211	5,415	6,002	41,1	44,4	50,49	0,06487	0,06739	0,07486
5	1255	1435	1733	4,954	5,294	5,965	39,88	43,02	49,76	0,06168	0,06589	0,0744
M	1283	1438	1722	5,211	5,256	5,796	40,77	43,13	49,45	0,06487	0,06541	0,07229
SD	20,55	22,5	57,09	0,1462	0,0703	0,1635	0,6529	0,6747	1,639	0,00182	0,00087	0,00204

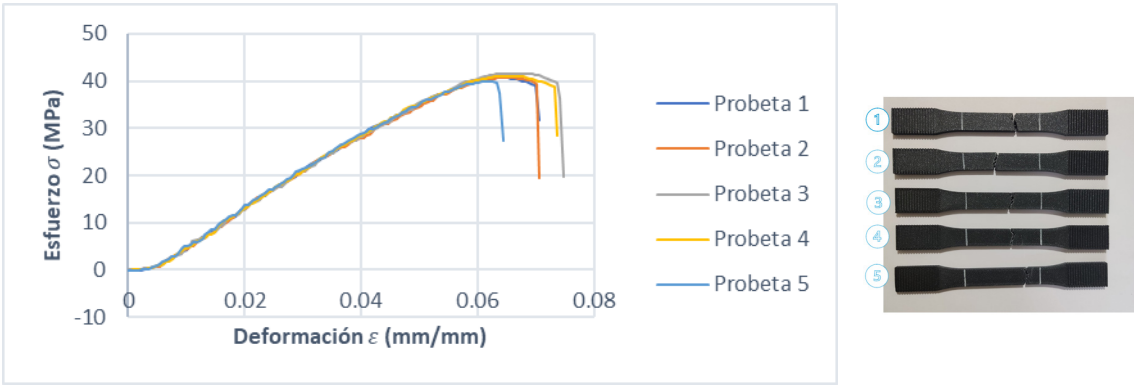

(a) Probetas SUNLU- Densidad de relleno 40 % - patrón cúbico

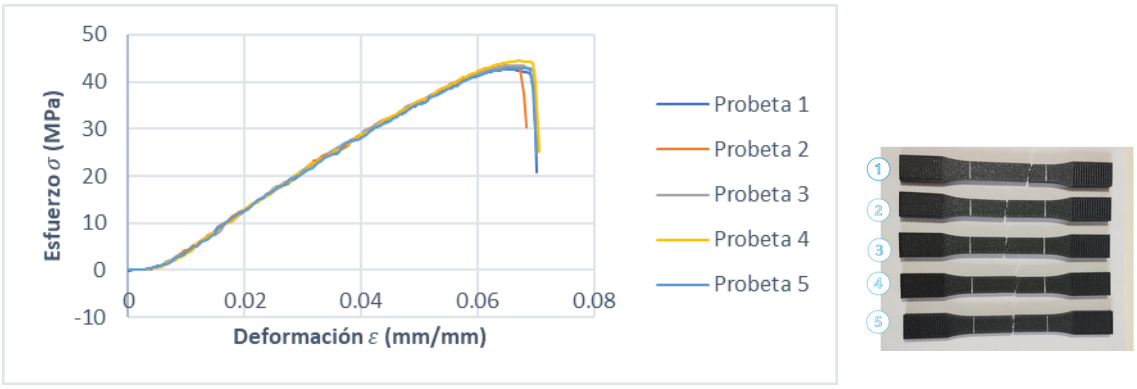

(b) Probetas SUNLU- Densidad de relleno 60 % - patrón cúbico

https://doi.org/10.56294/dm2025768

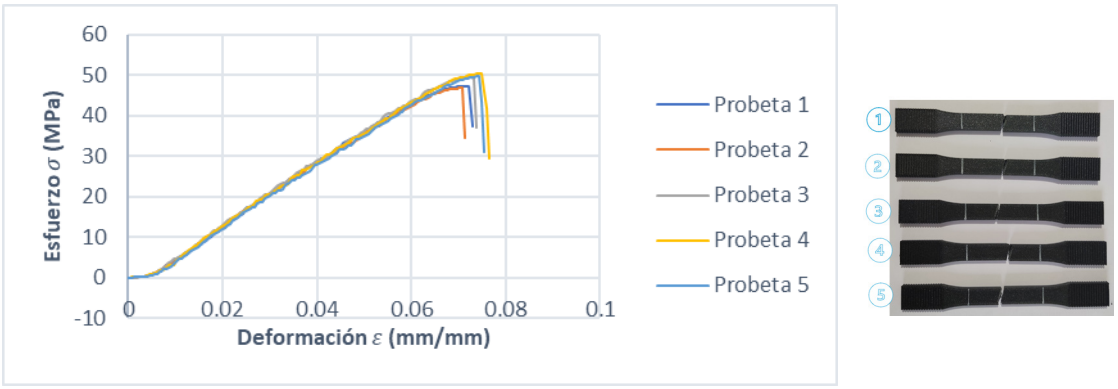

(c) Probetas SUNLU- Densidad de relleno 80 % - patrón cúbico

Figure 5. Stress [MPa] - Strain [mm/mm] graph of the Cubic PLA-FC (SUNLU) test specimens

Table 5. Results of tensile testing of PLA-FC Giroide (SUNLU) test pieces

P	Maximum Strength (N)			Extensión (mm)			Last-ditch effort (MPa)			Deformation (mm/mm)		
	40 %	60 %	80 %	40 %	60 %	80 %	40 %	60 %	80 %	40 %	60 %	80 %
1	1212	1474	1693	5,293	5,726	5,920	36,53	40,99	43,69	0,06593	0,07121	0,07395
2	1205	1478	1730	5,248	5,761	6,004	36,3	41,1	44,66	0,06537	0,07166	0,075
3	1216	1456	1716	5,333	5,628	6,094	36,64	40,51	44,29	0,06643	0,06999	0,07612
4	1241	1474	1735	5,349	5,636	6,137	37,4	41,01	44,77	0,06663	0,0701	0,07666
5	1222	1484	1729	5,295	5,762	6,076	36,81	41,27	44,62	0,06596	0,07167	0,0759
M	1216	1474	1729	5,295	5,726	6,076	36,64	41,01	44,62	0,06596	0,07121	0,0759
SD	13,71	10,2	17,01	0,0394	0,0663	0,0853	0,4132	0,2836	0,4389	0,000491	0,000825	0,001065

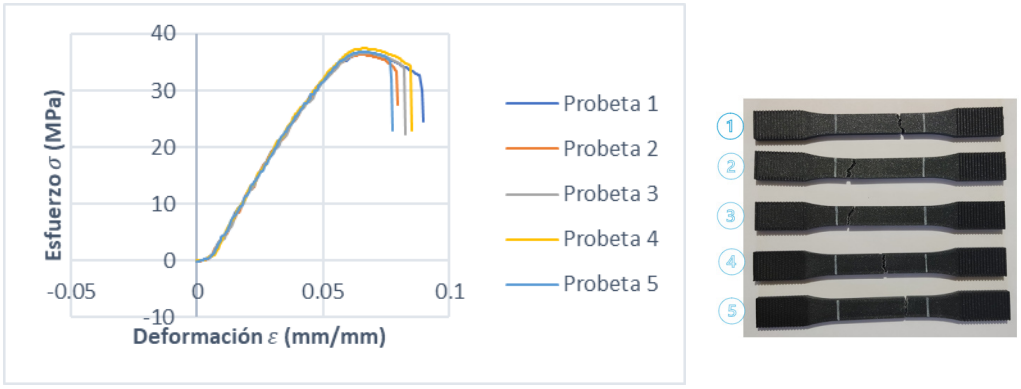

(a) Densidad de relleno 40 % - patrón giroide

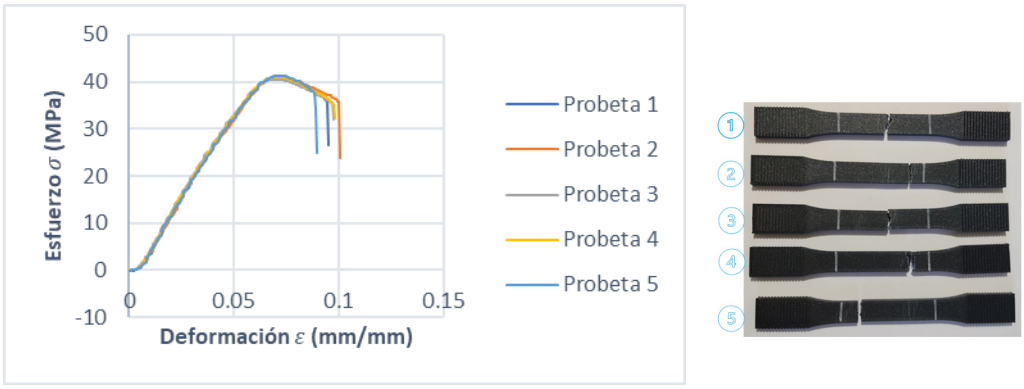

(b) Densidad de relleno 60 % - patrón giroide

https://doi.org/10.56294/dm2025768

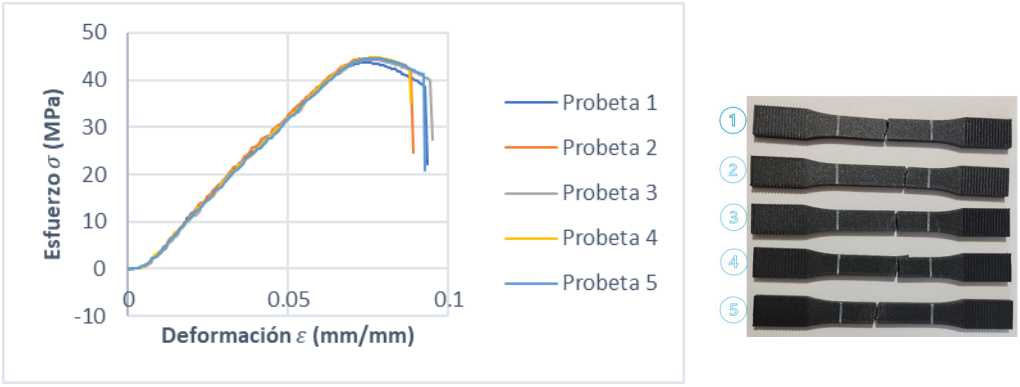

(c) Densidad de relleno 80 % - patrón giroide

Figure 6. Graph of Stress [MPa] – Strain [mm/mm] of the PLA-FC Giroide (SUNLU) test specimens

Table 6. Results of tensile testing of PLA-FC Triangular (SUNLU) test pieces

P	Maximum Strength (N)			Extensión (mm)			Last-ditch effort (MPa)			Deformation (mm/mm)		
	40 %	60 %	80 %	40 %	60 %	80 %	40 %	60 %	80 %	40 %	60 %	80 %
1	1200	1262	1321	4,876	4,904	5,335	37,85	38,68	36,66	0,06083	0,0613	0,07089
2	1189	1253	1353	4,794	4,843	5,346	37,51	38,41	37,55	0,05981	0,06054	0,07103
3	1193	1275	1310	4,884	4,952	5,139	37,62	39,06	36,36	0,06093	0,0619	0,06829
4	1183	1257	1342	4,756	4,917	5,206	37,3	38,54	37,25	0,05933	0,06146	0,06917
5	1178	1257	1302	4,788	4,779	5,212	37,16	38,52	36,14	0,05972	0,05973	0,06925
M	1189	1257	1321	4,794	4,904	5,212	37,51	38,54	36,66	0,05981	0,0613	0,06925
SD	8,523	8,299	21,36	0,0574	0,0684	0,0894	0,2688	0,2543	0,5927	0,00072	0,00086	0,00119

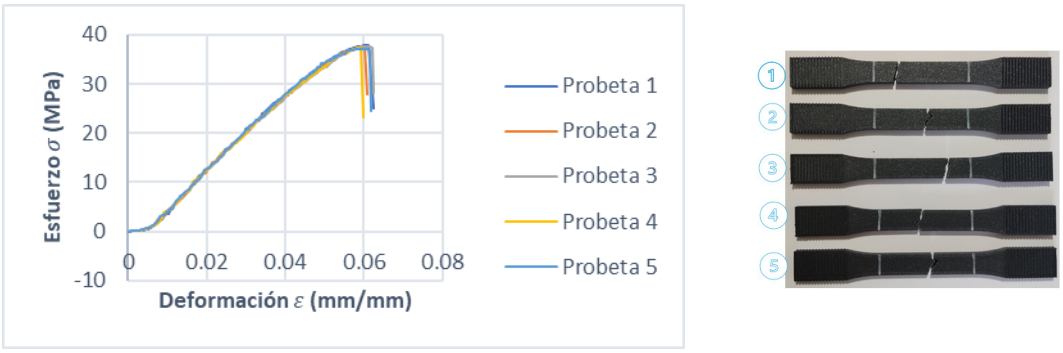

(a) Densidad de relleno 40 % - patrón triangular

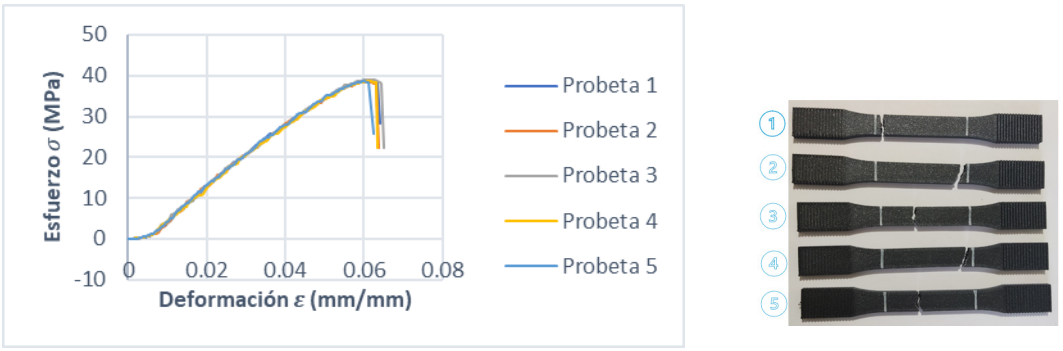

(b) Densidad de relleno 60 % - patrón triangular

https://doi.org/10.56294/dm2025768

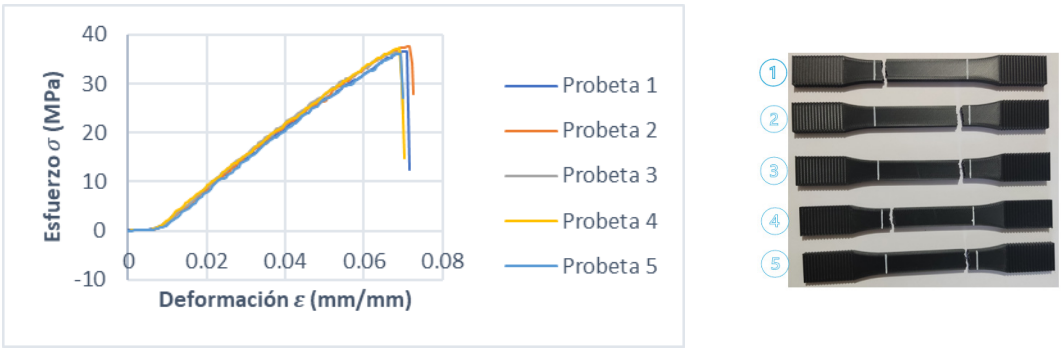

(c) Densidad de relleno 80 % - patrón triangular

Figure 7. Graph of Stress [MPa] – Strain [mm/mm] of PLA-FC Triangular (SUNLU) test specimens

Artillery PLA-FC test pieces

Table 7. Results of tensile testing of Cubic PLA-FC (Artillery) test specimens.

P	Maximum Strength (N)			Extensión (mm)			Last-ditch effort (MPa)			Deformation (mm/mm)		
	40 %	60 %	80 %	40 %	60 %	80 %	40 %	60 %	80 %	40 %	60 %	80 %
1	1201	1459	1670	5,537	5,837	6,247	38,17	43,76	47,93	0,07361	0,07748	0,08298
2	1229	1472	1652	5,765	5,878	6,215	39,04	44,13	47,43	0,07664	0,07802	0,08256
3	1171	1415	1642	5,503	5,794	6,378	37,20	42,42	47,15	0,07316	0,07692	0,08472
4	1213	1450	1654	5,580	5,916	6,373	38,56	43,49	47,48	0,07418	0,07853	0,08465
5	1182	1425	1696	5,467	5,747	6,464	37,55	42,73	48,70	0,07268	0,07629	0,08587
M	1201	1450	1654	5,537	5,837	6,373	38,17	43,49	47,48	0,07361	0,07748	0,08465
SD	23,40	23,78	21,16	0,1165	0,0666	0,1026	0,7436	0,7129	0,6077	0,00155	0,00088	0,00136

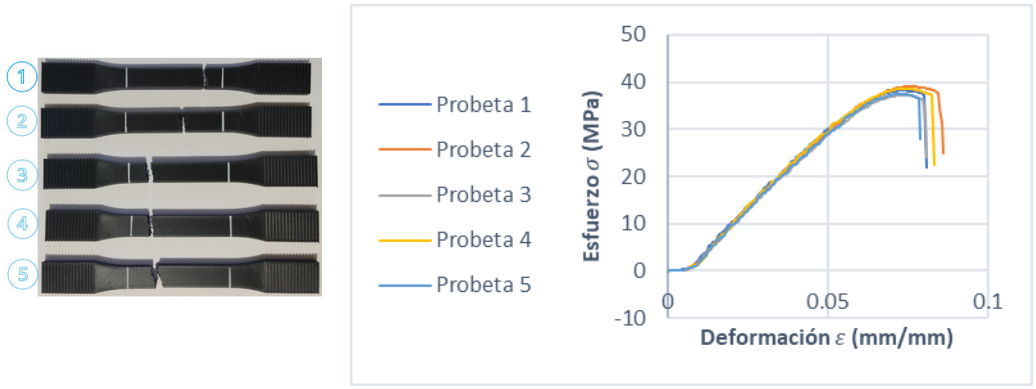

(a) Densidad de relleno 40 % - patrón cúbico

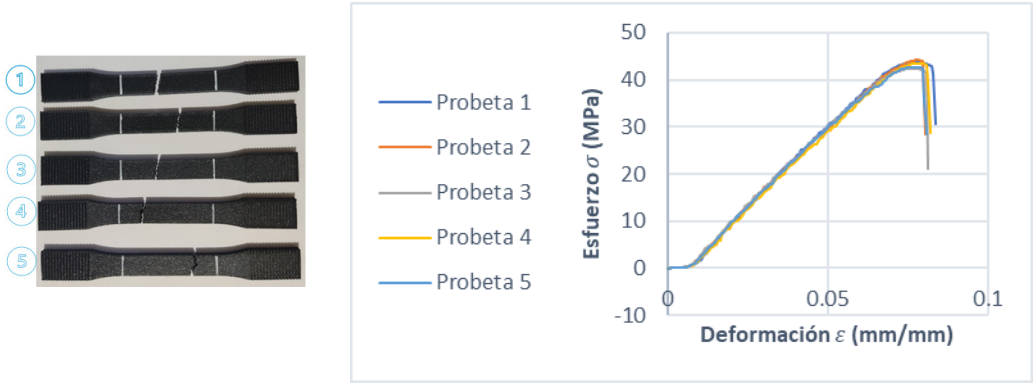

(b) Densidad de relleno 60 % - patrón cúbico

https://doi.org/10.56294/dm2025768

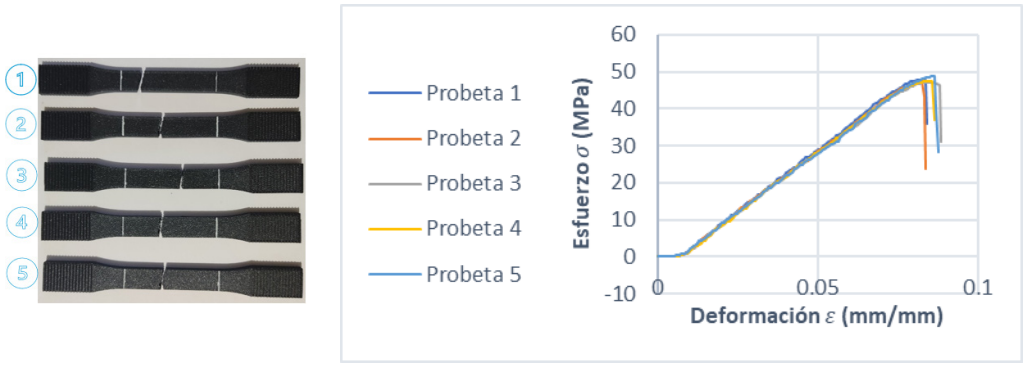

(c) Densidad de relleno 80 % - patrón cúbico

Figure 8. Stress [MPa] - Strain [mm/mm] graph of the Cubic PLA-FC (Artillery) test specimens

Tables 7, 8, 9 and figures 8, 9 and 10 show the results of the tensile test on the Artillery test pieces, with cubic, gyroid and triangular filling patterns, respectively.

Table 8. Results of tensile testing of PLA-FC Giroide (Artillery) test specimens

P	Maximum Strength (N)			Extensión (mm)			Last-ditch effort (MPa)			Deformation (mm/mm)		
	40 %	60 %	80 %	40 %	60 %	80 %	40 %	60 %	80 %	40 %	60 %	80 %
1	1202	1425	1682	5,705	6,087	6,587	36,23	39,65	43,41	0,07573	0,08096	0,08721
2	1260	1448	1671	5,888	6,134	6,416	37,97	40,28	43,13	0,07816	0,08158	0,08493
3	1077	1472	1621	5,831	6,294	6,299	32,46	40,95	41,84	0,07741	0,08371	0,08339
4	1170	1426	1631	5,704	6,132	6,415	35,25	39,66	42,08	0,07573	0,08156	0,08492
5	1172	1473	1668	5,717	6,386	6,591	35,32	40,97	43,05	0,07590	0,08493	0,08726
M	1172	1448	1668	5,717	6,134	6,416	35,32	40,28	43,05	0,07590	0,08158	0,08493
SD	66,33	23,53	27,01	0,08513	0,1271	0,1258	1,999	0,6546	0,6971	0,00113	0,00169	0,00167

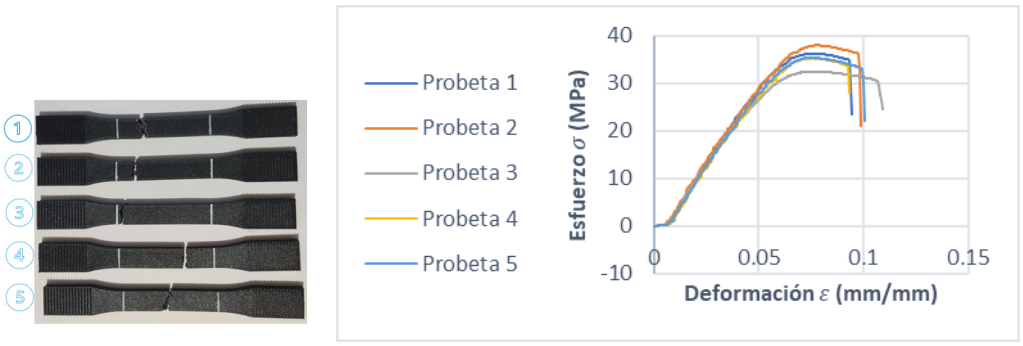

(a) Densidad de relleno 40 % - patrón giroide

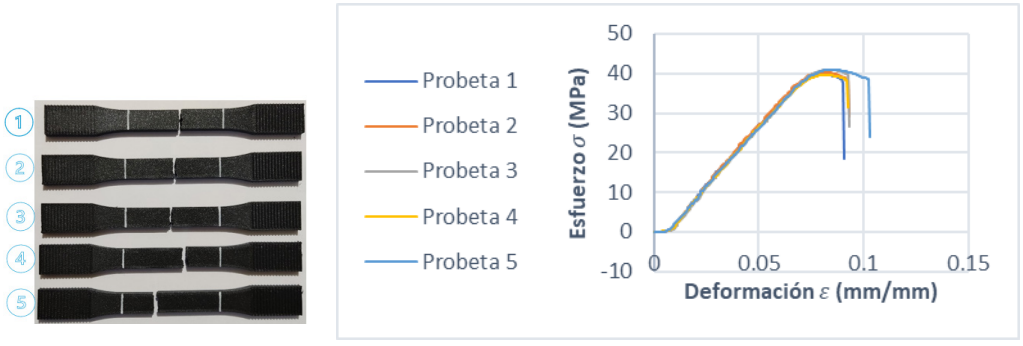

(b) Densidad de relleno 60 % - patrón giroide

https://doi.org/10.56294/dm2025768

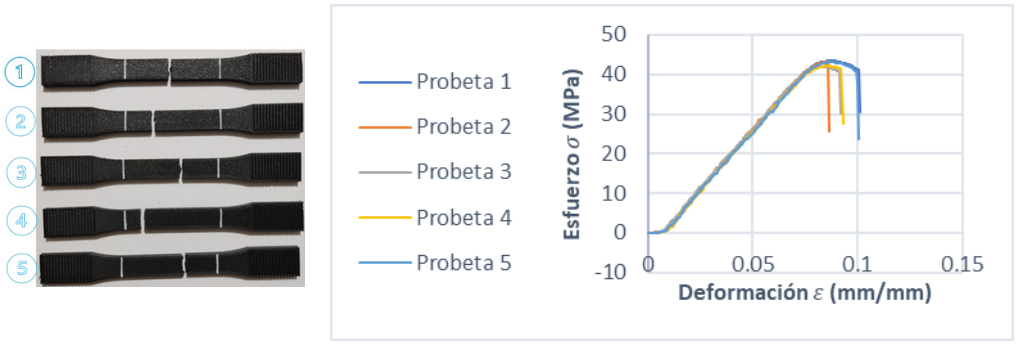

(c) Densidad de relleno 80 % - patrón giroide

Figure 9. Graph of Stress [MPa] – Strain [mm/mm] of the PLA-FC Giroide (Artillery) test specimens

The results of this group of test specimens are reflected in the table, which shows the mechanical properties of each specimen, such as ultimate tensile stress, ultimate strain, and modulus of elasticity.

Table 9. Results of tensile testing of PLA-FC Triangular Artillery test pieces

P	Maximum Strength (N)			Extensión (mm)			Last-ditch effort (MPa)			Deformation (mm/mm)		
	40 %	60 %	80 %	40 %	60 %	80 %	40 %	60 %	80 %	40 %	60 %	80 %
1	1139	1200	1430	5,289	5,164	5,546	35,91	36,78	39,70	0,06996	0,06817	0,07353
2	1091	1180	1397	5,218	5,202	5,299	34,39	36,16	38,77	0,06901	0,06867	0,07026
3	1115	1227	1437	5,289	5,382	5,473	35,16	37,62	39,88	0,06995	0,07105	0,07256
4	1096	1200	1456	5,164	5,163	5,579	34,57	36,76	40,41	0,06830	0,06816	0,07397
5	1115	1164	1413	5,299	5,032	5,494	35,18	35,66	39,21	0,07008	0,06644	0,07284
M	1115	1200	1430	5,289	5,164	5,494	35,16	36,76	39,70	0,06995	0,06817	0,07284
SD	18,99	24,03	22,65	0,059	0,126	0,109	0,599	0,736	0,629	0,00078	0,00166	0,00144

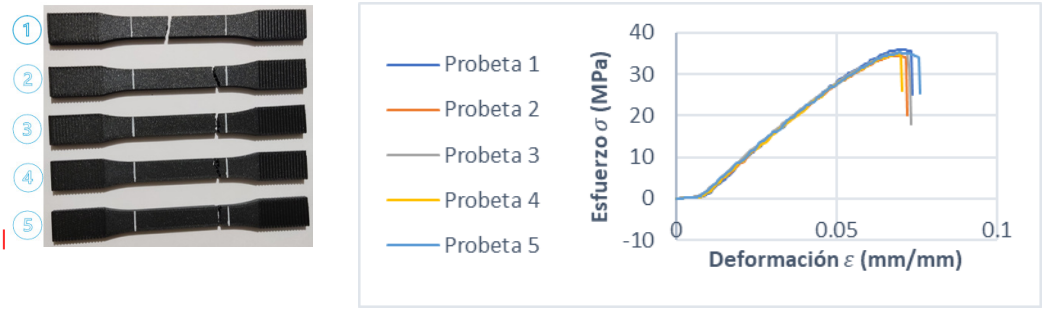

(a) Densidad de relleno 40 % - patrón triángular

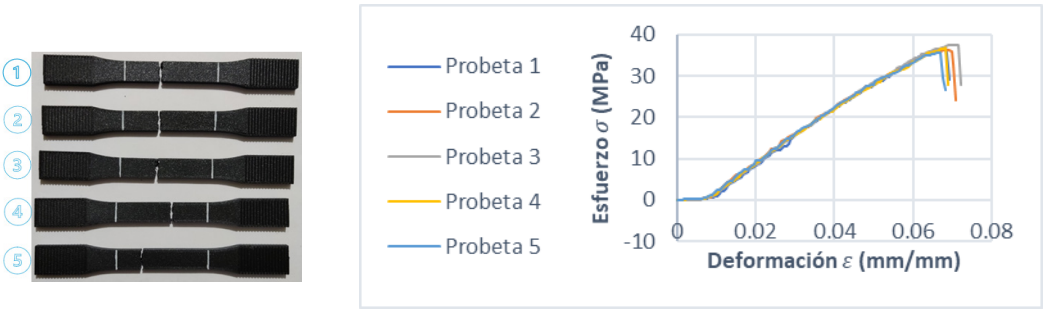

(b) Densidad de relleno 60 % - patrón triangular

https://doi.org/10.56294/dm2025768

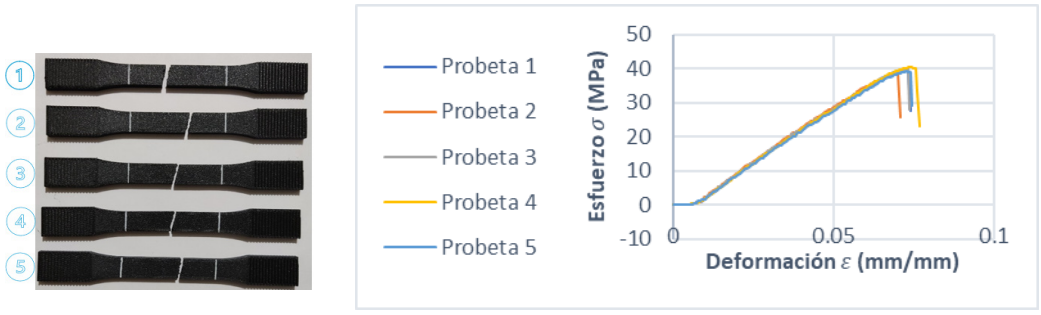

(c) Densidad de relleno 80 % - patrón triangular

Figure 10. Graph of Stress [MPa] – Strain [mm/mm] of the PLA-FC Triangular (Artillery) test pieces

Values representing the mechanical properties of PLA-FC

Table 10 shows the results obtained for the mechanical properties of ultimate tensile stress (), strain (), and Young's modulus () of the samples tested

Table 10. Summary of the mechanical properties of FC SUNLU and Artillery PLA

Fill pattern	Filling density	SUNLU			Artillery			Relative difference		
		S_u (MPa)	ε_u (mm/mm)	E (MPa)	S_u (MPa)	ε_u (mm/mm)	E (MPa)	S_u (MPa)	ε_u (mm/mm)	E (MPa)
Cubic	40 %	40,77	0,06487	803,5	38,17	0,07361	694,1	6,8 %	-11,9 %	15,8 %
	60 %	43,13	0,06541	827,8	43,49	0,07748	698,6	-0,8 %	-15,6 %	18,5 %
	80 %	49,45	0,07229	809,2	47,48	0,08465	679,3	4,1 %	-14,6 %	19,1 %
Gyroid	40 %	36,64	0,06596	732,9	35,32	0,07590	663,6	3,7 %	-13,1 %	10,4 %
	60 %	41,01	0,07121	750,6	40,28	0,08158	639,8	1,8 %	-12,7 %	17,3 %
	80 %	44,62	0,0759	735,0	43,05	0,08493	624,2	3,6 %	-10,6 %	17,8 %
Triangular	40 %	37,51	0,05981	783,8	35,16	0,06995	665,9	6,7 %	-14,5 %	17,7 %
	60 %	38,54	0,06130	785,7	36,76	0,06817	678,6	4,8 %	-10,1 %	15,8 %
	80 %	36,66	0,06925	651,2	39,70	0,07284	673,8	-7,7 %	-4,9 %	-3,4 %

DISCUSSION

Ultimate tensile stress

For better visualization, figure 11 shows the representative values of the ultimate tensile stress for each pattern and filling density of SUNLU and Artillery filaments.

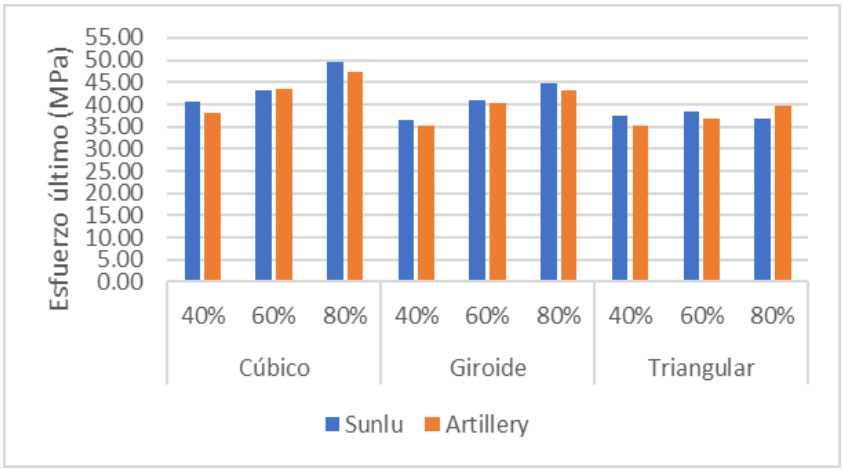

Figure 11. Comparison of ultimate stress [MPa] for each pattern and filling density

When comparing the cubic, gyroid, and triangular filling patterns with a density of 40 % of the SUNLU and Artillery brands, the cubic pattern of SUNLU offers the maximum tensile strength, with a value of 40,77 MPa, followed by the same pattern of the Artillery brand, with a value of 38,17 MPa.

https://doi.org/10.56294/dm2025768

When examining the results corresponding to the three filling patterns with a density of 60 % of the two filaments, it can be seen that the highest ultimate tensile strength is obtained with the cubic pattern of Artillery, whose value is 43,49 MPa, followed by the same filling pattern of the SUNLU filament, with a value of 43,13 MPa. The relative difference is minimal.

The results of the maximum ultimate tensile strength at 80 % density, considering the three filling patterns, show that the cubic SUNLU pattern allows for more excellent stability, with a value of 49,45 MPa, followed by the same Artillery pattern, with a value of 47,48 MPa.

When comparing the results, the cubic pattern allows for the greatest tensile strength for each filling density. In most cases, SUNLU's PLA-FC filament provides higher ultimate stress, except with the 60 % cubic and 80 % triangular filling patterns.

For designs where strength is the only important factor, the relative difference is sufficiently low (less than 8 %) for the cost to be more critical, so it is suggested that cheaper Artillery be used.

Young's modulus

The figure shows the representative Young's modulus values for each infill pattern and density of the two brands.

When comparing the three filling patterns with a density of 40 % of both brands, the cubic pattern of SUNLU offers a higher elastic modulus, with a value of 803,5 MPa, followed by the triangular pattern of the same brand, with a value of 783,8 MPa.

When analyzing the results corresponding to the density of 60 % of the three filling patterns, it can be seen that the cubic pattern of SUNLU has the highest elastic modulus, with a value of 827,8 MPa, followed by the triangular pattern of the same brand, which has a value of 785,7 MPa.

Regarding the highest elastic modulus with a density of 80 %, considering the three filling patterns, the cubic pattern of SUNLU has the highest modulus, with a value of 809,2 MPa, followed by the gyroid pattern of the same brand, with a value of 735 MPa.

When analyzing the results, it can be seen that the cubic filling pattern has a higher elastic modulus for each filling percentage. The maximum elastic modulus is presented in the cubic filling pattern at 60 % of SUNLU, followed by the cubic filling patterns at 80 % and 40 % of the same brand. In addition, it can be seen that in most cases, the SUNLU filament offers a higher Young's modulus, except for the triangular filling pattern at 80 %.

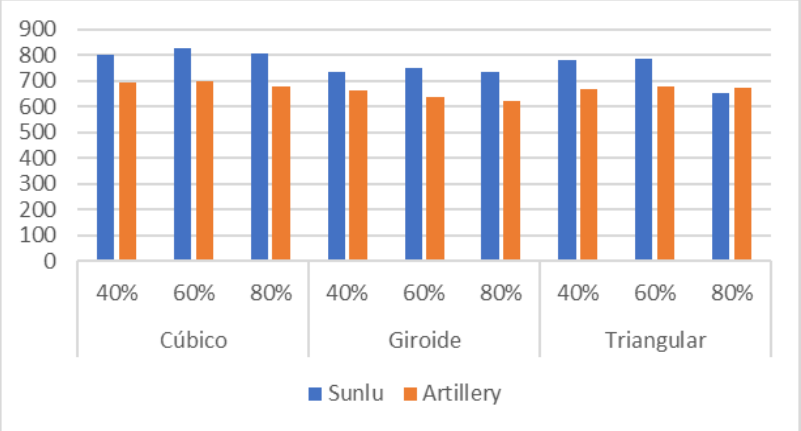

Figure 12. Comparison of the elastic modulus [MP] for each pattern and filling density

Deformation

Figure 13 shows the representative values of the ultimate deformation corresponding to each pattern and percentage of SUNLU and Artillery filament fill.

When comparing the results considering the three patterns with a density of 40 % of the two filaments, it can be seen that Artillery's gyroid pattern allows the most significant deformation with a value of 0,0759, followed by the cubic pattern of the same brand, whose value is 0,07361.

When comparing the filling patterns with a density of 60 %, the Artillery gyroid filling pattern offers the greatest deformation, with a value of 0,08158, followed by the cubic pattern of the same brand.

When analyzing the results corresponding to the 80 % density of each filling pattern, the Artillery gyroid pattern allows a deformation of 0,08493, followed by the cubic filling pattern of the same brand.

The greatest ultimate deformation occurs in the 80 % gyroid fill pattern of Artillery, followed by the 80 % cubic and 60 % gyroid fill patterns of the same brand of filament. In each case, the Artillery filament offers greater deformation compared to the SUNLU filament.

https://doi.org/10.56294/dm2025768

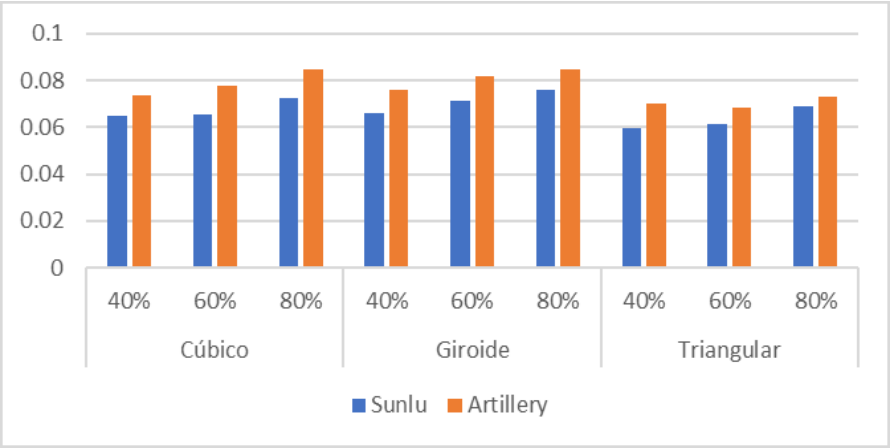

Figure 13. Comparison of the deformation [mm/mm] for each pattern and filling density

CONCLUSIONS

The research identified the necessary parameters for the tensile tests on the specimens printed using the FDM technique. The printing temperature, speed, density, and filling pattern suitable for characterization in carbon fiber-reinforced PLA specimens were determined. Careful adjustment of these parameters is essential for consistent and reliable results.

Based on the ASTM D638 14 standard, Tensile tests carried out on SUNLU and Artillery brand CF PLA specimens revealed the filling pattern and density that offers the best mechanical properties for the different conditions.

The maximum ultimate stress is presented with the cubic filling pattern and 80 % filling density of SUNLU's PLA FC filament, followed by the exact configuration of Artillery's PLA FC filament.

The Artillery PLA FC filament allows for more significant deformation in each configuration, which is more noticeable with the cubic and gyroid fill patterns with their respective fill percentages.

The highest Young's modulus is presented with the cubic pattern at 80 %, followed by the same fill pattern with a density of 60 % of the SUNLU filament. In most cases, the SUNLU filament has an elastic modulus greater than 15 % compared to the Artillery filament.

Given the above, it is concluded that both materials offer advantages in some mechanical properties, and the respective selection will depend on the manufacturer's requirements.

BIBLIOGRAPHIC REFERENCES

1. Muhamedagic K, Berus L, Potočnik D, Cekic A, Begic-Hajdarevic D, Cohodar Husic M, et al. Effect of Process Parameters on Tensile Strength of FDM Printed Carbon Fiber Reinforced Polyamide Parts. Applied Sciences. 2022 Jun 14;12(12):6028.

2. Pagés-Llobet A, Espinach FX, Julián F, Oliver-Ortega H, Méndez JA. Effect of Extruder Type in the Interface of PLA Layers in FDM Printers: Filament Extruder Versus Direct Pellet Extruder. Polymers (Basel). 2023 Apr 24;15(9):2019.

3. Singh J, Goyal KK, Sharma R. Impact of FDM variables on the tensile property of 3D printed CF-PLA parts. Mater Today Proc. 2024;113:60–7.

4. Zonoobi MA, Haghshenas Gorgani H, Javaherneshan D. Experimental investigation and multi-objective optimization of FDM process parameters for mechanical strength, dimensional accuracy, and cost using a hybrid algorithm. Scientia Iranica. 2023 Jun 20;0(0):0–0.

5. Ambade V, Rajurkar S, Awari G, Yelamasetti B, Shelare S. Influence of FDM process parameters on tensile strength of parts printed by PLA material. International Journal on Interactive Design and Manufacturing (IJIDeM). 2025 Jan 7;19(1):573–84.

6. Calles AF, Carou D, Ferreira RTL. Experimental Investigation on the Effect of Carbon Fiber Reinforcements in the Mechanical Resistance of 3D Printed Specimens. Applied Composite Materials. 2022 Jun 1;29(3):937–52.

7. Venkateswar Reddy M, Hemasunder B, Mahadevapa Chavan P, Dish N, Paul Savio A. Study on the significance of process parameters in improvising the tensile strength of FDM printed carbon fibre reinforced PLA. Mater Today Proc. 2023 Jul;

8. Ajay Kumar M, Khan MS, Mishra SB. Effect of fused deposition machine parameters on tensile strength of printed carbon fiber reinforced PLA thermoplastics. Mater Today Proc. 2020;27:1505–10.

9. Maqsood N, Rimašauskas M. Characterization of carbon fiber reinforced PLA composites manufactured by fused deposition modeling. Composites Part C: Open Access. 2021 Mar;4.

10. Díaz-Rodríguez JG, Pertúz-Comas AD, González-Estrada OA. Mechanical properties for long fibre reinforced fused deposition manufactured composites. Compos B Eng. 2021 Apr 15;211.

11. Chacón JM, Caminero MA, Núñez PJ, García-Plaza E, García-Moreno I, Reverte JM. Additive manufacturing of continuous fibre reinforced thermoplastic composites using fused deposition modelling: Effect of process parameters on mechanical properties. Compos Sci Technol. 2019 Sep 8;181:107688.

12. Durga Rajesh KV, Ganesh N, Yaswanth Kalyan Reddy S, Mishra H, Teja Naidu TMVPS. Experimental research on the mechanical characteristics of fused deposition modelled ABS, PLA and PETG specimens printed in 3D. Mater Today Proc. 2023 Jul;

13. Santos JD, Fernández A, Ripoll L, Blanco N. Experimental Characterization and Analysis of the In-Plane Elastic Properties and Interlaminar Fracture Toughness of a 3D-Printed Continuous Carbon Fiber-Reinforced Composite. Polymers (Basel). 2022 Jan 27;14.

14. Lau HY, Hussin MS, Hamat S, Abdul.Manan MS, Ibrahim M, Zakaria H. Effect of kenaf fiber loading on the tensile properties of 3D printing PLA filament. Mater Today Proc. 2023 Mar;

15. Ambade V, Rajurkar S, Awari G, Yelamasetti B, Shelare S. Influence of FDM process parameters on tensile strength of parts printed by PLA material. International Journal on Interactive Design and Manufacturing (IJIDeM). 2023 Aug 7;

16. Algarni M. Tensile strength and strain behavior study and modeling of PLA printed parts with optimized AM parameters. Procedia Structural Integrity. 2023;51.

FINANCING

The authors did not receive any funding for the development of the research.

CONFLICT OF INTEREST

The authors declare that there is no conflict of interest

AUTHORSHIP CONTRIBUTION

Conceptualization: Arley Chuquín, Brizeida Gámez, Marco Naranjo, David Ojeda.
Data curation: Arley Chuquín.
Formal analysis: Arley Chuquín, Bizeida Gámez.
Research: Arley Chuquín, Brizeida Gámez.
Methodology: Marco Naranjo, David Ojeda.
Project administration: Brizeida Gámez.
Resources: Arley Chuquín, Brizeida Gámez, Marco Naranjo, David Ojeda.
Supervision: Marco Naranjo and David Ojeda.
Validation: Arley Chuquín, Brizeida Gámez.
Visualization: Arley Chuquín, Brizeida Gámez.
Writing - original draft: Arley Chuquín, Brizeida Gámez.
Writing - review and editing: Brizeida Gámez.